Revue des Composites et des Matériaux Avancés-Journal of Composite and Advanced Materials
Vol. 36, No. 1, February, 2026, pp. 125-132
Journal homepage: http://iieta.org/journals/rcma

Impact of Bending Angle on Ovalization and Thickness Distribution in Mandrel-Free Copper Tube Bending: An Experimental and Finite Element Analysis

Mohammed S. Jabbar, Ammar M. Saleh, Adil S.Jaber*

College of Production Engineering and Metallurgy, University of Technology, Baghdad 10011, Iraq

Corresponding Author Email: adil.s.jaber@uotechnology.edu.iq

https://doi.org/10.18280/rcma.360112

Received: 1 December 2025
Revised: 27 January 2026
Accepted: 16 February 2026
Available online: 28 February 2026

Keywords:
bending angle, thin-walled copper tube, ovalization, thickness variation, mandrel-free bending, finite element analysis, tube forming defects, material behavior

ABSTRACT

Mandrel-free tube bending is widely used in industries due to its low tooling cost, but it introduces defects like wall thickness variation and ovalization, especially in thin-walled tubes. This study investigates the effect of bending angle on these defects in C12200 copper tubes. The effects were explored through both experimental and finite element analysis (FEA). Copper tubes with an outer diameter of 16 mm and a wall thickness of 0.8 mm were bent at 90°, 110°, and 130° bending angles. The results revealed that smaller bending angles increased defect occurrence, with a 5% thinning and 10.63% thickening at 90°. Larger angles reduced thickness variation and ovalization, enhancing tube cross-section stability. The experimental and numerical results showed good agreement, with discrepancies under 5%. This research provides practical guidelines for minimizing defects during mandrel-free tube bending, helping optimize the manufacturing process for thin-walled copper tubes.

1. INTRODUCTION

Bending is considered one of the most important forming technologies. The first bending machine was patented over 100 years ago, and since then, the technique has become widely adopted [1]. The primary challenge addressed in this study is conducting the tube bending process without a mandrel despite its critical role in preventing ovalization, flattening of the tube section, and inward collapse. As the bending process begins, the material at the bending zone confined between the outer and inner radius undergoes continuous variation in stresses and strains. As the bending radius decreases, the strain neutral layer shifts away from its position of original geometrical neutral axis as seen in Figure 1 [2, 3]. At the initial stage, deformation is primarily elastic till the forming forces reach the yielding point. The plastic flow begins as the forming process continues, with the plastic zone expanding through the tube cross-section and along the tube length axis. This continues until the tube bend radius coincides with that of the die, at which point the plastic deformation process ends as depicted in Figure 2 [4].

Anekar et al. [5] studied the prediction of effective stress and thickness distribution of 6061 Al-alloy, where a finite element analysis (FEA) was employed to build a parametric tube analysis under the assumption of ovalization of the cross-section and bending is symmetrical along the vertical axis. Fang et al. [6] focus on demonstrating the connection between tube factors and stress-strain and thickness variation using an analytical model; an FEA was utilized to investigate process and geometrical parameters. Zhang and Hu [7] developed FE models to represent the bending and springback process in order to improve the pressure die, which leads to decease the reduction of wall thickness and tube axial elongation. Michalczyk et al. [8] conducted a numerical and experiential study to develop a new method to reduce ovalization in addition to flattening as much as possible by using different profile bending roll impressions during three-point bending of EN-AW 6060 aluminum alloy and 16Mo3 boiler steel tubes with an outer diameter of 20 mm and 2 mm thickness at a low bend radius. Elyasi et al. [9] introduce a new method in rotary draw bending by utilizing a bending die with varying curvature to deform the tube from a big to a small bend radius and use pressurized fluid as a mandrel. The results show good enhancement in thinning and thickening when using this method. Liu and Liu [10] studied the difference in accuracy of finite element models according to three yield criteria in defining anisotropic characteristics of heterogeneous rectangular tubes through research and experiments. The results reveal that Hill 48 produces the most accurate description. The study [11] utilized experiments and the finite element method to investigate the mechanical properties of tubes with D/t ratios in the range of 40 and 97 under a combination of bending loads and axial compression. The study [12] proposed a diameter adjustable mandrel (DAM) that relies on multiple contact points to be adapted to tubes with different diameters of AISI 304L tubes with an inner diameter = 40–56 mm. The study [13] conducted a parametric study using FEA, and then validated FEA using the Digital Image Correlation technique to study the effect of three ratios between the dimension parameters of the tube's section: width-to-height, height-to-thickness, and width-to-thickness, on this mechanism. The study [14] conducted a comparative

study between compression bending and rotary draw bending in terms of springback, cross section compression and widening, cross section shape and wall thinning/thickening using aluminum alloy 6060-T4 round tubes with diameter of 60 mm and 3 mm wall thickness.

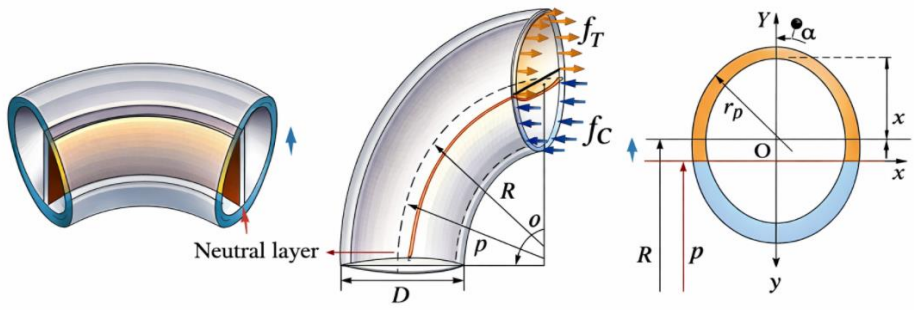

Figure 1. Geometrical positions of tube bending [2]

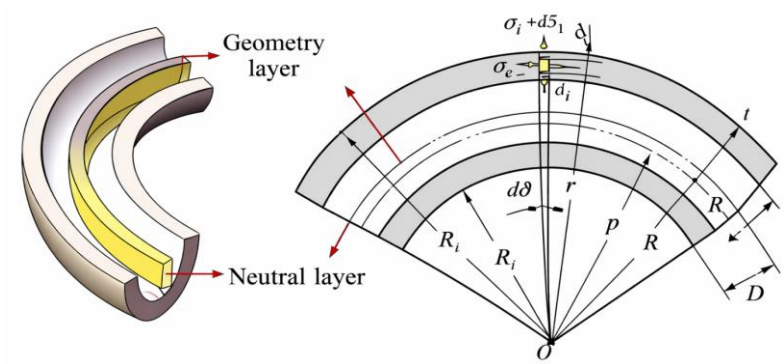

Figure 2. The bend terms and deformation region [5]

While other recent studies have focused on reducing bending defects through the use of tooling or additional supports (e.g., modified rolls or using pressurized mandrels), this research focuses on isolating the bending angle as the primary factor influencing the formation of bent C12200 Copper tubing without the use of mandrels during ram bending. This work establishes a new causal relationship between the specific plastic behavior of the material, the redistribution and ovalization of thicknesses during the bending process and how these factors contribute to potential failure during actual service conditions within the product. In addition to identifying defects, this combined experimental-Finite Element (FE) method allows us to predict the magnitude of defect(s) resulting from a given bending angle while also quantifying the uncertainty associated with each key variable. Thus, it provides manufacturers with specific recommendations on how to manage copper tube manufacturing processes without requiring additional complexities associated with specialized tooling.

2. METHODOLOGY

2.1 Variation of wall thickness

The change in wall thickness (Figure 3) is considered one of the major defects in tube bending according to the status of compressive stress and tensile stress at the inner and outer bend radius, respectively, causing thickening and thinning [15, 16]. These variations in thickness, both on the interior and exterior of the tube, can lead to wrinkling, wall thinning, and a reduction in strength, especially at the outer bend radii during service [17, 18].

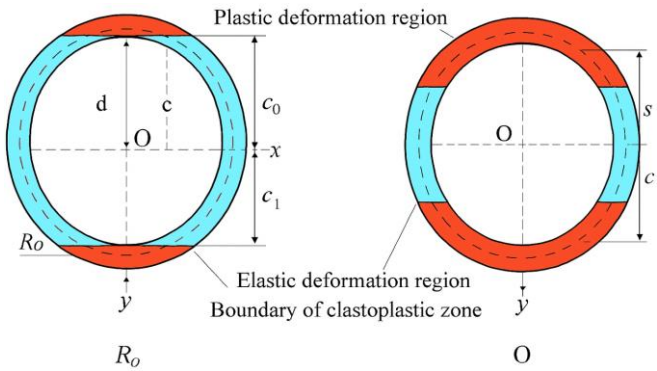

Figure 3. The state of tensile and compression regions [17]

Thinning ratio is known as the percent value of the differences between tube thickness and minimum thickness divided by tube wall thickness, as represented in Eq. (1):

$$th = \frac{t - t_{min}}{t} \quad (1)$$

where, t and t_{min} are the thickness and minimum thickness in mm, respectively.

On the other hand, the thickening ratio represents the percent value of the differences between tube maximum thickness and tube thickness divided by tube wall thickness as presented in Eq. (2).

$$th_k = \frac{t - t_{max}}{t} \quad (2)$$

where, t and t_{max} are the thickness and maximum thickness in

mm, respectively [18, 19].

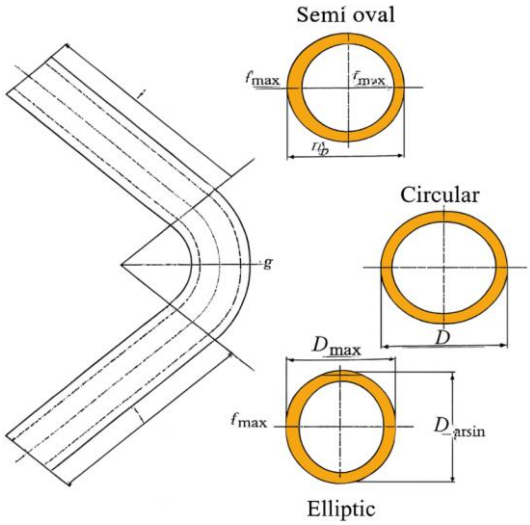

Figure 4. Ovality during tube bending [5]

2.2 Ovalization

The cross-section of the tube during plastic deformation starts to reshape from circular to oval due to the rotation of tube's surfaces around the neutral axis, as shown in Figure 4 [4]. These phenomena become more obvious during the deformation of low wall thickness tubes and bending at a small bend radius [20].

Ovality percentage could be calculated using the following Eq. (3).

$$Ovality = \frac{D_{max} - D_{min}}{Dm} \quad (3)$$

where, D_{max}, D_{min}, and D_m are the maximum, minimum, and mean diameter after the bending process in mm [16].

3. EXPERIMENTAL PROCEDURE

3.1 Tooling and equipment

In this work, an ASTM B280 cooper tube (C12200-DHP) with a dimension of 25 mm in length, 0.8 mm thickness, and 16 mm diameter samples were used as seen in Figure 5. Figure 6 shows the true stress- strain curve for the used samples and Table 1 illustrates the chemical and mechanical properties of used copper tubes (C12200-DHP). A hard plastic die of a fix bend radius was used to bend copper tubes (Figure 7) with WDW-200E Comprehensive Test Machine.

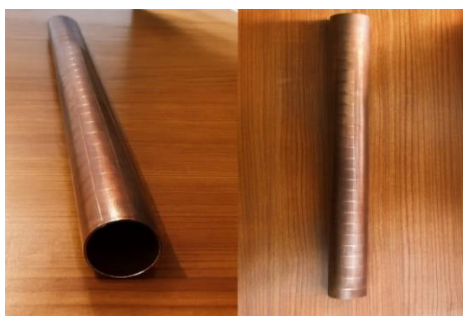

Figure 5. The photographs for the test specimens

Table 1. Mechanical and chemical properties of copper tube.

Mechanical Properties	Density	8.92	g/cm^3
	Tensile strength	205	MPa
	Elongation	40	%
	Yield Strength	60	MPa
	Young's modulus	120000	MPa
Chemical Composition	Copper	99.95	wt%
	phosphorus	0.004-0.012	wt%

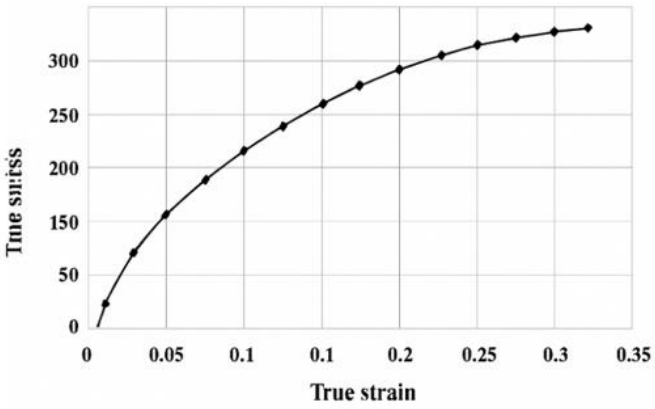

Figure 6. The true stress-truestrain for test specimens

Figure 7. The die used in this study

3.2 Bending procedure

The bending process was done by employing the ram bending method by preparing a specific setup and using the WDW-200E Comprehensive Test Machine to complete the bending operation, as illustrated in Figure 8. The copper tubes were bent in three bending angles, which are 130º, 110º, and 90º. The testing process was carried out at a speed of 50 mm/min.

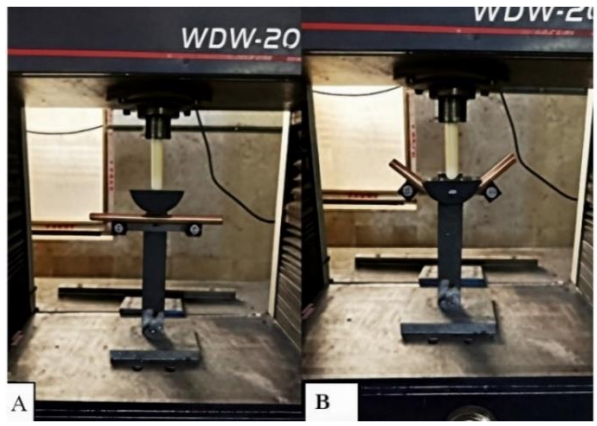

Figure 8. The photograph for the bending set, A) Initial arrangement, B) Final bending

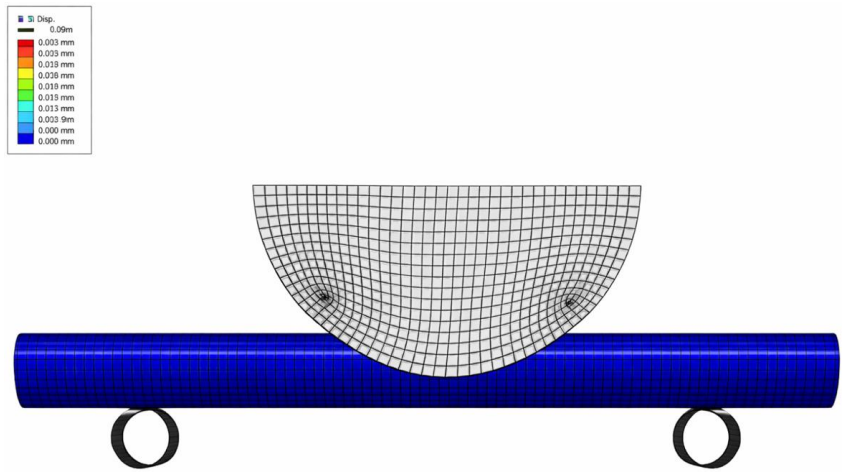

Figure 9. The finite element (FE) model used in this work

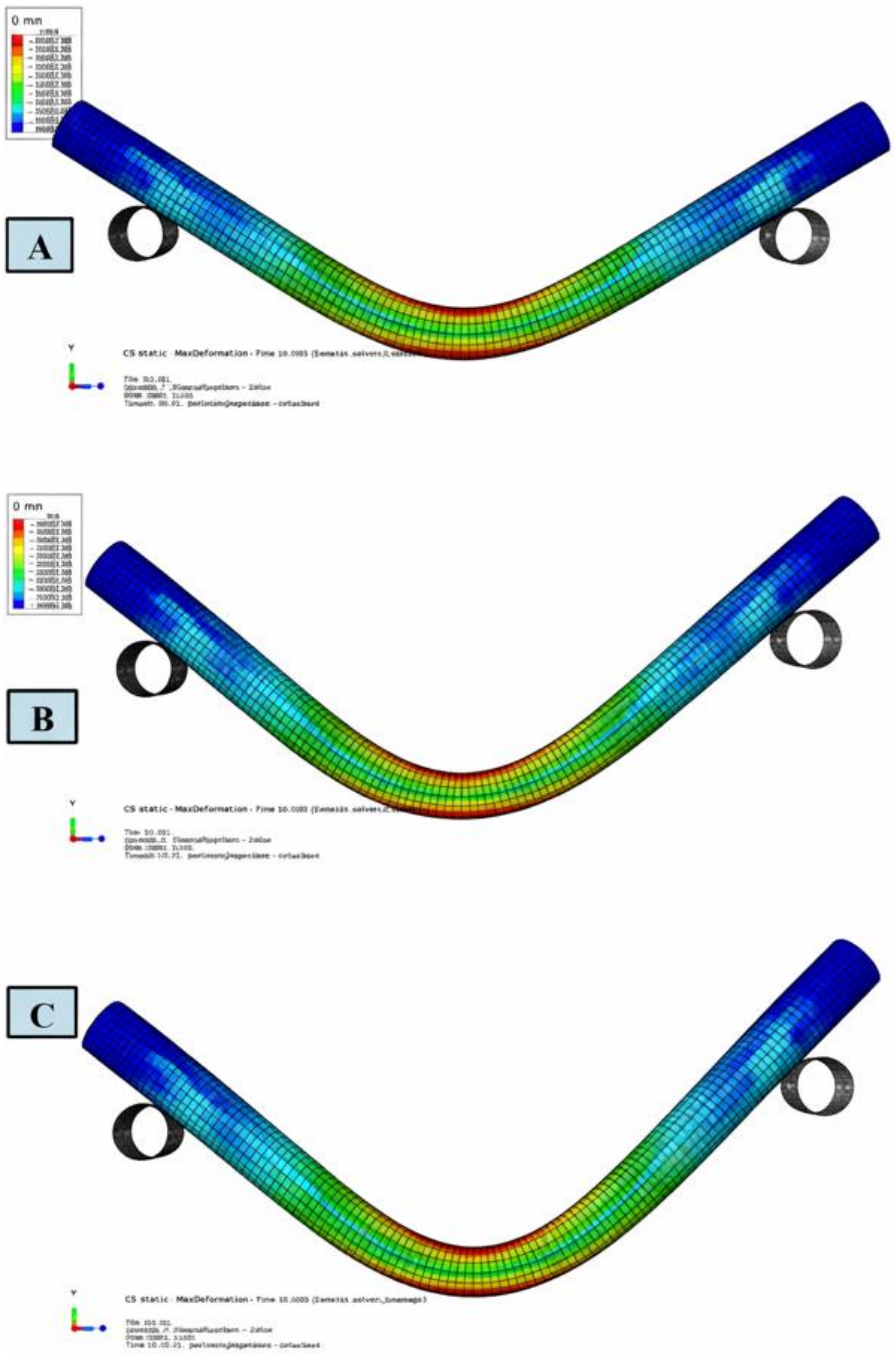

Figure 10. Complete bended model for the specimens, A) 130º, B) 110º, and C) 90º

4. NUMERICAL ANALYSIS

The numerical analysis was conducted using Abaqus/Explicit 6.14. The model employed C3D8R (8-node, 3D, first-order brick element with reduced integration and hourglass control) elements, generated using A hex-dominated meshing technique with a sweep algorithm. A global element size of 2 mm was specified, resulting in the mesh shown in Figure 9. A dynamic explicit solution scheme was adopted to simulate the large deformation and, complex contact conditions inherent to the bending process. Kinetic interactions (frictional contact) with friction coefficient of 0.1 between the tube and tooling components, to capture realistic forming behavior. Figure 10 illustrate the shape of test specimens after FE simulation is completed.

5. RESULTS AND DISCUSSION

5.1 Thickness distribution behavior

The results indicate that numerical analysis and the experimental validation are in stronge agreement and follow the same trend. Regarding thinning and thickening behavior, the maximum thinning and thickening occurred in the 90º bending zone, where the thinning ratio reaches 5.00% both experimentally and numerically, while the thickening ratio reaches 10.63% experimentally and 9.00% numerically. For the 110º and 130º angles, the thinning ration were 4% and 2.5% (numerically vs. experimentally) at 110º, and 3.13% and 1.50% (numerically vs. experimentally) at 130º. The thickening ratio were approximately 6.87% and 9.5% (numerically vs. experimentally) at 110º, and 6.5% and 6.25% (numerically vs. experimentally) at 130º.

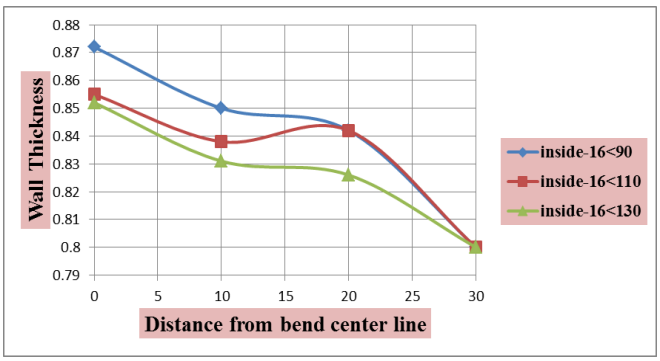

(A)

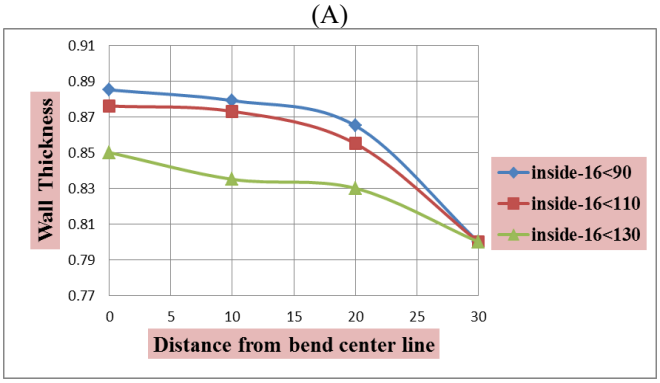

(B)

Figure 11. Thickening behavior for bended specimens at three angles 90º, 110º, and 130º, A) Numerically, and B) Experimentally

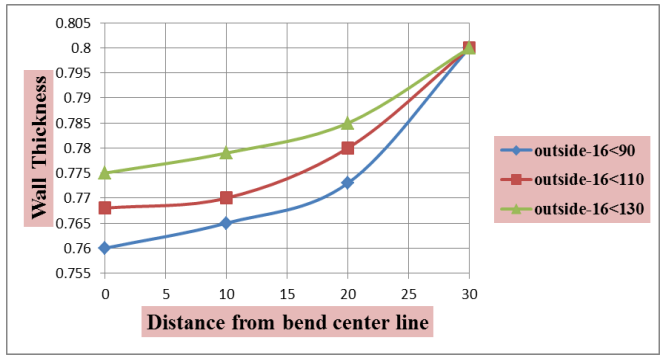

(A)

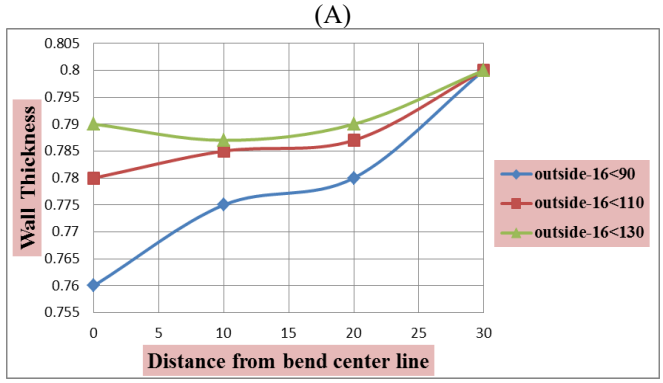

(B)

Figure 12. Thinning behavior for bended specimens at three angles 90º, 110º, and 130º, A) Numerically, and B) Experimentally

Figures 11 and 12 illustrate the thickening and thinning behavior measured from the bend centerline. This behavior is caused by tensile and compressive stresses generate stretching and pushing forces at the interior and exterior of bend area. These forces increase as the bend angle decreases, leading to thinning in the inner zone and thickening, with a little buckle -in the outer zone. In other words, the compressive stresses concentrated in the interior of the bend center and tensile stresses concentrated at the exterior of the bend center.

5.2 Ovality

The results reveal that the ovalization phenomenon increases as the bending angles decrease. It can be observed that the value of major axes increases while the value of minor axes decreases with smaller bending angles, and vice versa, as shown in Figure 13. This behavior can be attributed to several factors, including material type, bending angles, and wall thickness, etc. However, the key factor is the imbalance in stress distribution that develops in the tube walls during bending.

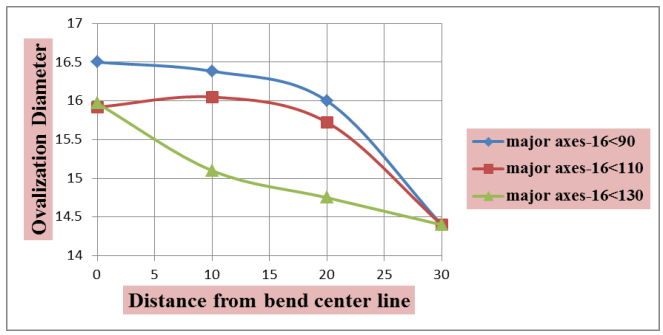

(A)

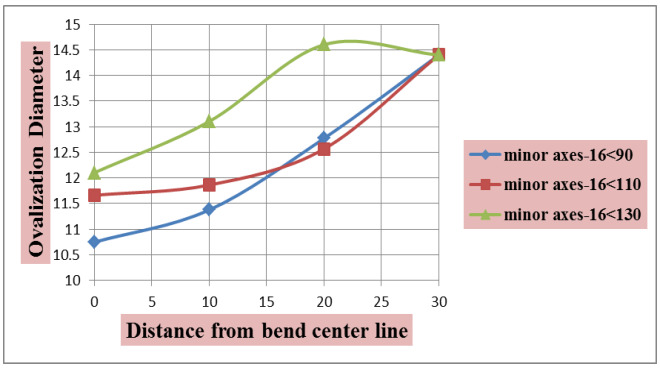

(B)

Figure 13. Diameters of bent specimens at 90°, 110°, and 130° bending angles: A) Major axes, B) Minor axes (simulation)

This imbalance leads to the loss of original circular cross-section, particularly when the bending is performed without a mandrel or internal support. Additionally, radial forces push the tube outward along the outer bend radius and pull it inward along the inner bend radius. The imbalance between these forces is a major contributor to ovalization. Figure 14 demonstrates the ovulation behavior for the three angles numerically.

5.3 Simulation–experiment discrepancy

With only a few variations in magnitude, the numerical results were found to closely match the experimental trends. For the 90° bending angle, the thickening ratio was slightly underestimated in the simulation (9% compared to the experimentally measured 10.63%), resulting in a difference of approximately 1.63 percentage points, or a relative error of roughly 15%. In contrast, the thinning ratio was exactly matched (approximately 5% in both cases). At the 110° and 130° bending angles, the thickening and thinning variations were mostly between 1% and 3%. Ovalization was observed to increase as the bending angle decreased, reaching around 42.26% in the simulation at 90°. Due to the idealized contact conditions and the lack of the initial tube ovality in the model, it was anticipated that the computational and experimental ovalization results would differ slightly, with an average uncertainty of ± 8–12%. These aberrations were primarily caused by idealizations in the numerical model. The capability of simplified isotropic elasto-plastic material law utilized to simulate the tube material properties is not adequately suitable for capturing the complex multiaxial hardening behavior encountered during bending. Additionally, the friction value has assumed to be constant at 0.1 in the simulation situation, while it is found fluctuating locally, leading to inaccuracy estimated ± 5–10% to the predictions of wall tube thickness.

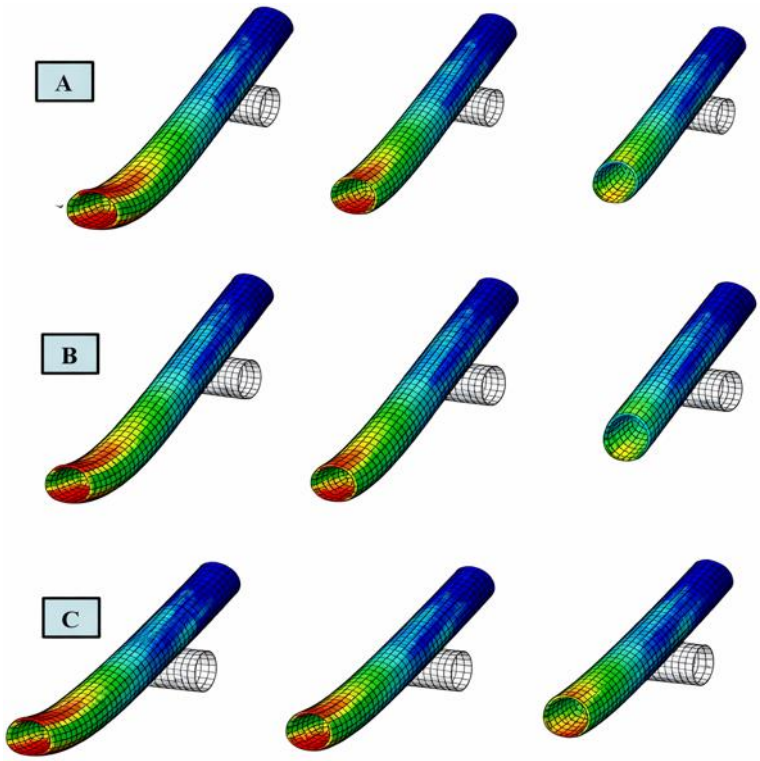

Figure 14. Ovalization behavior of deformed cross-sectional shape after bending process completed for three angles, A) 90º, B) 110º, and C) 130º

5.4 Contribution in context of recent research

This study provides a perspective that focuses on experimental and geometrical factors as a complement to advanced studies on tube bending. Most of the recent studies focused on complex tooling [8, 9] or complicated constitutive models to minimize defects. This work results showed that for bending without mandrel of ductile C12200 copper, merely increasing the bending angle from 90° to 130° reduces ovalization by more than 50% and improves the uniformity of thickness. This establishes a straightforward, cost-effective design rule: high bending angles improve cross-section stability for unsupported bending of thin-walled tubes. These findings provide useful guidelines for this typical industrial scenario by producing manufacturers with a key geometric factor to optimize before exploring more complex solutions.

6. CONCLUSIONS

This work shows the effect of bending angles on thickness variation and ovalization in ram bending without a mandrel, for copper tubes experimentally and by simulation. The results illustrate that the bending angles have a strong influence on forming quality. The small angles like 90º show the highest defects and thinning of about 5%, thickening reaching 10.63% experimentally, and considerable ovalization of about 42.26%. As the bending angle increased to over 110°, the defects reduced noticeably, which refers to the enhancement in structural stability of the tube cross-section.

From a practical engineering perspective, the results propose that high bending angles, especially above 110º are more appropriate for bending without a mandrel when the main target is to stabilize or reduce wall thickness variation and ovalization. The simulation predictions are in good agreement with experimental results, with most discrepancies remaining within a few percent, confirming the capability of the FE model to capture the main deformation behavior.

However, this work was restricted to one type of copper alloy, fixed geometry, and forming at room temperature conditions, with simple hypotheses in the simulation model. For future works, the researchers should consider various materials, temperature conditions, and tube dimensions, as well as more advanced modeling and surface integrity analysis to further optimize the process and improve defect prediction.

REFERENCES

[1] Gillanders, J. (1994). Pipe and Tube Bending Manual. Croydon Group.

[2] Yan, J., Yang, H., Zhan, M., Li, H. (2010). Forming limits under multi-index constraints in NC bending of aluminum alloy thin-walled tubes with large diameters. Science China Technological Sciences, 53: 326-342. https://doi.org/10.1007/s11431-009-0331-x

[3] Saleh, A.M., Jaber, A.S., Jabbar, M.S. (2025). Layer adhesion investigation of three dimension printed parts by controlling the environment temperature. Advances in Science and Technology Research Journal, 19(3): 74-83. https://doi.org/10.12913/22998624/197333

[4] Khodayari, G. (2008). Pre-forming: Tube rotary draw bending and preflattening/crushing in hydroforming. In Hydroforming for Advanced Manufacturing, pp. 181-201.

[5] Anekar, N., Nimbalkar, S., Shinde, H., Narwade, G., Nimje, S. (2019). Parametric analysis of tube during bending operation. International Journal of Innovative Technology and Exploring Engineering, 8(10): 1793-1799. https://doi.org/10.35940/ijitee.J9186.0881019

[6] Fang, J., Ouyang, F., Lu, S.Q., Wang, K.L., Min, X.G., Xiao, B.T. (2021). Wall thinning behaviors of high strength 0Cr21Ni6Mn9N tube in numerical control bending considering variation of elastic modulus. Advances in Mechanical Engineering, 13(5): 1-14. 10.1177/16878140211021241

[7] Zhang, H., Hu, Y. (2022). Influence of pressure die's boosting on forming quality in bending process of thin-walled tube. International Journal of Pressure Vessels and Piping, 196: 104612. https://doi.org/10.1016/j.ijpvp.2022.104612

[8] Michalczyk, J., Gontarz, A., Wiewiórowska, S., Winiarski, G. (2023). Mandrel-free bending of tubes with small radii – A theoretical and experimental study. Advances in Science and Technology Research Journal, 17(4): 189-205. https://doi.org/10.12913/22998624/169883

[9] Elyasi, M., Khatir, F.A., Ghadikolaee, H.T., Modanloo, V. (2024). Experimental investigation and numerical simulation of the effect of type of bending die on the quality of tube forming in rotary draw bending process. International Journal of Lightweight Materials and Manufacture, 7(2): 233-247. https://doi.org/10.1016/j.ijlmm.2023.10.005

[10] Liu, H., Liu, Y. (2021). Cross section deformation of heterogeneous rectangular welded tube in rotary draw bending considering different yield criteria. Journal of Manufacturing Processes, 61: 303-310. https://doi.org/10.1016/j.jmapro.2020.11.015

[11] Jin, S., Cheng, P., Saneian, M., Bai, Y. (2021). Mechanical behavior of thin tubes under combined axial compression and bending. Thin-Walled Structures, 159: 107255. https://doi.org/10.1016/j.tws.2020.107255

[12] Li, J., Wang, Z., Zhang, S., Lin, Y., Wang, L., Sun, C., Tan, J. (2023). A novelty mandrel supported thin-wall tube bending cross-section quality analysis: A diameter-adjustable multi-point contact mandrel. The International Journal of Advanced Manufacturing Technology, 124(11): 4615-4637. https://doi.org/10.1007/s00170-023-10838-y

[13] Rincon-Davila, D., Alcalá, E., Martin, A. (2022). Theoretical–experimental study of the bending behavior of thin-walled rectangular tubes. Thin-Walled Structures, 173: 109009. https://doi.org/10.1016/j.tws.2022.109009

[14] Tronvoll, S.A., Ma, J., Welo, T. (2023). Deformation behavior in tube bending: A comparative study of compression bending and rotary draw bending. The International Journal of Advanced Manufacturing Technology, 124(3): 801-816. https://doi.org/10.1007/s00170-022-10433-7

[15] Mohammed, A.R., Jawad, W.K. (2024). Practical test and FEA to evaluation of the thickness distribution for octagonal cup generated by deep drawing. AIP Conference Proceedings, 3002: 080022. https://doi.org/10.1063/5.0205959

[16] Ma, J., Li, H., Fu, M.W. (2021). Modelling of springback in tube bending: A generalized analytical approach. International Journal of Mechanical Sciences, 204: 106516. https://doi.org/10.1016/j.ijmecsci.2021.106516

[17] Mohammed, A.R., Jawad, W.K. (2024). Octagonal shape design through the use of FEA and experimental methods are created in deep drawing. AIP Conference Proceedings, 3002: 060016. https://doi.org/10.1063/5.0205958

[18] Păunoiu, V., Tabib A.K., Maier, C. (2015). Bendenability limits in three-roll tube bending. Annals of ”Dunarea de Jos” University of Galati, Fascicle V, Technologies in machine building [Internet]. https://www.gup.ugal.ro/ugaljournals/index.php/tmb/article/view/1478.

[19] Michael, T., Veerappan, A., Shanmugam, S. (2012). Effect of cross section on collapse load in pipe bends subjected to in-plane closing moment. International Journal of Engineering, Science and Technology, 3(6): 247-256. https://doi.org/10.4314/ijest.v3i6.20

[20] Sasidharan, S., Arunachalam, V., Subramaniam, S. (2017). Ramifications of structural deformations on collapse loads of critically cracked pipe bends under in-plane bending and internal pressure. Nuclear Engineering and Technology, 49(1): 254-266. https://doi.org/10.1016/j.net.2016.09.001